antioxidants

MDPI

Article

In *Escherichia coli* Ammonia Inhibits Cytochrome bo_3 But Activates Cytochrome *bd*-I

Elena Forte [1,*], Sergey A. Siletsky [2] and Vitaliy B. Borisov [2,*]

[1] Department of Biochemical Sciences, Sapienza University of Rome, P.le A. Moro 5, 00185 Rome, Italy
[2] Belozersky Institute of Physico-Chemical Biology, Lomonosov Moscow State University, Leninskie Gory, 119991 Moscow, Russia; siletsky@belozersky.msu.ru
* Correspondence: elena.forte@uniroma1.it (E.F.); bor@belozersky.msu.ru (V.B.B.)

Abstract: Interaction of two redox enzymes of *Escherichia coli*, cytochrome bo_3 and cytochrome *bd*-I, with ammonium sulfate/ammonia at pH 7.0 and 8.3 was studied using high-resolution respirometry and absorption spectroscopy. At pH 7.0, the oxygen reductase activity of none of the enzymes is affected by the ligand. At pH 8.3, cytochrome bo_3 is inhibited by the ligand, with 40% maximum inhibition at 100 mM $(NH_4)_2SO_4$. In contrast, the activity of cytochrome *bd*-I at pH 8.3 increases with increasing the ligand concentration, the largest increase (140%) is observed at 100 mM $(NH_4)_2SO_4$. In both cases, the effector molecule is apparently not NH_4^+ but NH_3. The ligand induces changes in absorption spectra of both oxidized cytochromes at pH 8.3. The magnitude of these changes increases as ammonia concentration is increased, yielding apparent dissociation constants K_{dapp} of 24.3 ± 2.7 mM $(NH_4)_2SO_4$ (4.9 ± 0.5 mM NH_3) for the Soret region in cytochrome bo_3, and 35.9 ± 7.1 and 24.6 ± 12.4 mM $(NH_4)_2SO_4$ (7.2 ± 1.4 and 4.9 ± 2.5 mM NH_3) for the Soret and visible regions, respectively, in cytochrome *bd*-I. Consistently, addition of $(NH_4)_2SO_4$ to cells of the *E. coli* mutant containing cytochrome *bd*-I as the only terminal oxidase at pH 8.3 accelerates the O_2 consumption rate, the highest one (140%) being at 27 mM $(NH_4)_2SO_4$. We discuss possible molecular mechanisms and physiological significance of modulation of the enzymatic activities by ammonia present at high concentration in the intestines, a niche occupied by *E. coli*.

Keywords: bacteria; redox enzymes; respiratory oxidases; ammonia; environmental stressor

Citation: Forte, E.; Siletsky, S.A.; Borisov, V.B. In *Escherichia coli* Ammonia Inhibits Cytochrome bo_3 But Activates Cytochrome *bd*-I. *Antioxidants* **2021**, *10*, 13. https://dx.doi.org/10.3390/antiox10010013

Received: 20 November 2020
Accepted: 21 December 2020
Published: 25 December 2020

1. Introduction

Cytochrome bo_3 and cytochrome *bd*-I are terminal oxidases in the aerobic respiratory chain of *Escherichia coli* [1]. Both enzymes catalyze the same redox reaction, the electron transfer from ubiquinol-8 to molecular oxygen giving rise to ubiquinone-8 and water [2,3]. In both cases this reaction is coupled to the formation of an electrochemical proton gradient across the bacterial cytoplasmic membrane [4–6]. Nevertheless, the bo_3 oxidase shows a higher energy transduction efficiency than the *bd*-I oxidase because the former utilizes the proton pumping mechanism [4,7].

The 3D structures of the proteins were determined [8–10]. Each one is composed of four different subunits, however the cytochromes are structurally and evolutionarily unrelated. Cytochrome bo_3 is a member of type A-1 of the heme-copper oxidase superfamily [11–16]. It carries the ubiquinol binding site, two hemes, *b* and o_3, and a copper ion [17]. The latter, denoted Cu_B, forms together with heme o_3 a binuclear site in which the oxygen chemistry takes place. The *bd*-type oxidases form their own family, distinct from the heme-copper superfamily, and the *E. coli* cytochrome *bd*-I belongs to the L subfamily of that family [3,18]. The *bd*-I enzyme has no copper but contains a binding site for ubiquinol and three hemes, b_{558}, b_{595}, and *d*. Heme *d* serves as the site for the O_2 reduction reaction.

Cytochrome bo_3 and cytochrome *bd*-I are expressed in *E. coli* under normal and low aeration conditions, respectively [19]. This is consistent with the fact that bo_3 is a low-oxygen-affinity oxidase [20], whereas *bd*-I is a high-oxygen-affinity oxidase [21]. The

oxidases bo_3 and *bd*-I differ in their sensitivity to small ligands. Cytochrome bo_3 was shown to be much more sensitive to NO, H_2S and cyanide than cytochrome *bd*-I [22–27]. The situation seems to be the opposite only in relation to the inhibition of the oxidases by CO [28]. The *bd*-I enzyme also contributes to the protection of *E. coli* against oxidative and nitrosative stress, playing an active antioxidant role in scavenging peroxynitrite and H_2O_2 [29–32]. The fact that the *bd*-type oxidase endows microbes with resistance to the toxic small molecules may explain why this respiratory enzyme is so abundant among bacterial pathogens. Since the *bd* protein is found only in prokaryotes, it may become a suitable target for next-generation antimicrobials [33].

E. coli is a consistent inhabitant of the intestinal tract of humans and warm-blooded animals. It is known that the intestines, particularly the large intestine lumen, reveal very high concentrations of ammonia, being in the millimolar range [34]. This raises the question of whether this ligand affects the functioning of the bacterial terminal oxidases. In this work, we have examined the effect of ammonia on oxygen consumption of cytochromes bo_3 and *bd*-I of *E. coli* (at the level of both isolated enzymes and intact cells) and absorption spectra of the enzymes. To our knowledge, the effect of this ligand on a terminal quinol oxidase has never been studied.

2. Materials and Methods

2.1. Reagents and Purification of Cytochromes bd-I and bo_3 from E. coli

Tris Base was purchased from Fisher BioReagents. Other chemicals were purchased from Sigma-Aldrich. Cytochromes *bd*-I and bo_3 were isolated from the *E. coli* strains GO105/pTK1 and GO105/pJRhisA, respectively, as described by [35–37]. In the case of cytochrome *bd*-I, the fractions with an absorbance ratio of $A_{412}/A_{280} \geq 0.7$ eluted from a DEAE Sepharose Fast Flow anion exchange column were pooled and concentrated [36]. Cytochrome bo_3 preparations were a kind gift of Marina Verkhovskaya (University of Helsinki). Being a His-tagged fusion protein, cytochrome bo_3 was purified by immobilized metal chelate affinity chromatography on Ni-NTA Agarose. The fractions eluted from the column containing pure four-subunit cytochrome bo_3 were pooled and concentrated [37]. The sample quality was evaluated by measuring enzyme activity and absorption spectra. All prepared samples showed high oxygen reductase activity (V_{max} of about 150 mol O_2/mol cytochrome *bd*-I/s and 60 mol O_2/mol cytochrome bo_3/s in the presence of the electron donor/mediator couple 10 mM dithiothreitol (DTT) and 0.25 mM 2,3-dimethoxy-5-methyl-6-(3-methyl-2-butenyl)-1,4-benzoquinone (Q_1) at pH 7.0) and characteristic absorption spectra both "as prepared" and dithionite-reduced. The concentration of cytochrome *bd*-I was determined from the dithionite reduced-*minus*-"as prepared" difference absorption spectra using $\Delta\varepsilon_{628\text{-}607}$ of 10.8 mM^{-1} cm^{-1} [38]. Cytochrome bo_3 concentration was estimated from the Soret absorption band of the oxidized enzyme using ε_{407} of 182 mM^{-1} cm^{-1} [39].

2.2. Measurement Techniques and Assay Conditions.

O_2 consumption of cytochromes *bd*-I and bo_3 was measured using an Oxygraph-2k high-resolution respirometer (Oroboros Instrument, Innsbruck, Austria) equipped with two 1.5-mL chambers. UV-visible absorption spectra were recorded in an Agilent Cary 60 UV-Vis spectrophotometer. Assays were performed at 25 °C in 100 mM Tris-phosphate (pH 8.3) or 100 mM potassium phosphate (pH 7.0) buffer containing 0.1 mM EDTA, 2.5 µg/mL catalase, 10 mM DTT, 0.25 mM Q_1, and either 0.05% *N*-lauroyl-sarcosine (cytochrome *bd*-I) or 0.02% dodecyl-β-D-maltoside (cytochrome bo_3). The concentrations of cytochrome bo_3 and cytochrome *bd*-I used in the oxygraphic measurements were 20 nM and 7.8 nM at pH 8.3, and 12 nM and 3.9 nM at pH 7.0 respectively. In the spectroscopic measurements, the concentrations of cytochrome bo_3 and cytochrome *bd*-I were 4.8 µM and 3.2 µM respectively. The pH of the stock solutions of $(NH_4)_2SO_4$ and K_2SO_4 was adjusted to the desired values (8.3 or 7.0). To generate the reduced state of cytochrome bo_3 or cytochrome *bd*-I, a few grains of solid sodium dithionite were added. The oxidized state of cytochrome *bd*-I was produced by incubating the "as isolated" enzyme with 33 µM tetrachloro-1,4-benzoquinone

for 10 min [40]. To remove excess oxidant, the sample was centrifuged at 4 °C and the yellow pellet discarded.

2.3. Data Analysis

Data analysis was carried out using Origin (OriginLab Corporation). To compare the $(NH_4)_2SO_4$ titration data obtained in oxygraphic and spectroscopic experiments, they were fitted to the standard hyperbolic equation $y = A_{max} \cdot x/(K_{dapp} + x)$ using a built-in approximation function ("hyperbola function") in "advanced fitting tool" in the Origin program. A_{max} and K_{dapp} parameters were allowed to vary. K_{dapp} is an *apparent* dissociation constant. In oxygraphic experiments, A_{max} is either a theoretical maximum percent inhibition (cytochrome bo_3) or a theoretical maximum percent activity (cytochrome *bd*-I). In spectroscopic experiments, A_{max} is a theoretical maximum absorption change. *R*-square (R^2) and standard deviation reported by the Origin program are shown in the figure legends. Since the high ionic strength may affect the activity of an enzyme [41], in order to take into account this possible effect, K_2SO_4 at the same concentration was added to the enzyme for each condition as a control.

3. Results

3.1. Effect of $(NH_4)_2SO_4$ on O_2 Reductase Activity of *E. coli* Cytochrome bo_3

The effect of $(NH_4)_2SO_4$ on the O_2-reductase activity of the isolated cytochrome bo_3 from *E. coli* was examined by measuring the O_2 consumption rates before and after addition of the effector at pH 8.3 or 7.0. Figure 1A shows that at pH 8.3 the addition of 50 mM $(NH_4)_2SO_4$ rapidly inhibits the O_2 reductase activity of cytochrome bo_3 by 51%. To take into account the effect of increasing ionic strength on enzyme activity, K_2SO_4 was added to the oxidase under the same conditions as a control. As shown in Figure 1A, 50 mM K_2SO_4 at pH 8.3 inhibits cytochrome bo_3 to a much lesser extent (by 18%). At pH 7.0 $(NH_4)_2SO_4$ does not inhibit the O_2 reductase activity of the bo_3 enzyme (Figure 1B). Figure 1C shows that with the increase in $(NH_4)_2SO_4$ concentration, the inhibitory effect at pH 8.3 is progressively increased. The maximum inhibition observed (after subtraction of the corresponding control value with K_2SO_4) was 40% at 100 mM $(NH_4)_2SO_4$.

We also studied the effect of $(NH_4)_2SO_4$ on O_2 consumption by *E. coli* mutant cells expressing cytochrome bo_3 as a single terminal oxidase. Supplementary Figures S1B and S2 show that within the limits of the experimental error the addition of $(NH_4)_2SO_4$ up to 27 mM at pH 8.3 caused no significant change in the respiration of the intact cells.

3.2. Effect of $(NH_4)_2SO_4$ on Absorption Spectra of *E. coli* Cytochrome bo_3

The finding that $(NH_4)_2SO_4$ can inhibit cytochrome bo_3 pushed us to explore the effect of ammonia on absorption spectra of the isolated cytochrome bo_3. Figure 2A shows the spectral changes induced by the addition of $(NH_4)_2SO_4$ at millimolar concentrations to the oxidized cytochrome bo_3 at pH 8.3. The ammonia-induced spectrum showed a red shift of the enzyme Soret band with a maximum at 416 nm and a minimum at 400 nm. In the visible spectrum, some weak intensity broad bands were displayed, the most pronounced of which was a band with a minimum around 630 nm. The spectral changes caused by the ligand are possibly due to its binding to the heme o_3-Cu_B binuclear site. The observed changes could be also due to a small reduction of the enzyme. However, the reduced-minus-oxidized spectrum in the Soret region of cytochrome bo_3 showed a maximum at 428–430 nm [39,42] rather than 416 nm. The magnitude of the Soret spectral changes increased as $(NH_4)_2SO_4$ concentration was increased (Figure 2B). Analysis of the titration curve yields K_{dapp} of 24.3 ± 2.7 mM $(NH_4)_2SO_4$ and the value for maximum absorption change at 416–400 nm A_{max} of 22.1 ± 0.6 $mM^{-1}cm^{-1}$. It has to be noted that the titration profile (Figure 2B) is similar to that for the plot of percent inhibition versus $(NH_4)_2SO_4$ (Figure 1C). The addition of $(NH_4)_2SO_4$ to the dithionite-reduced cytochrome bo_3 under identical conditions brought about no spectral change.

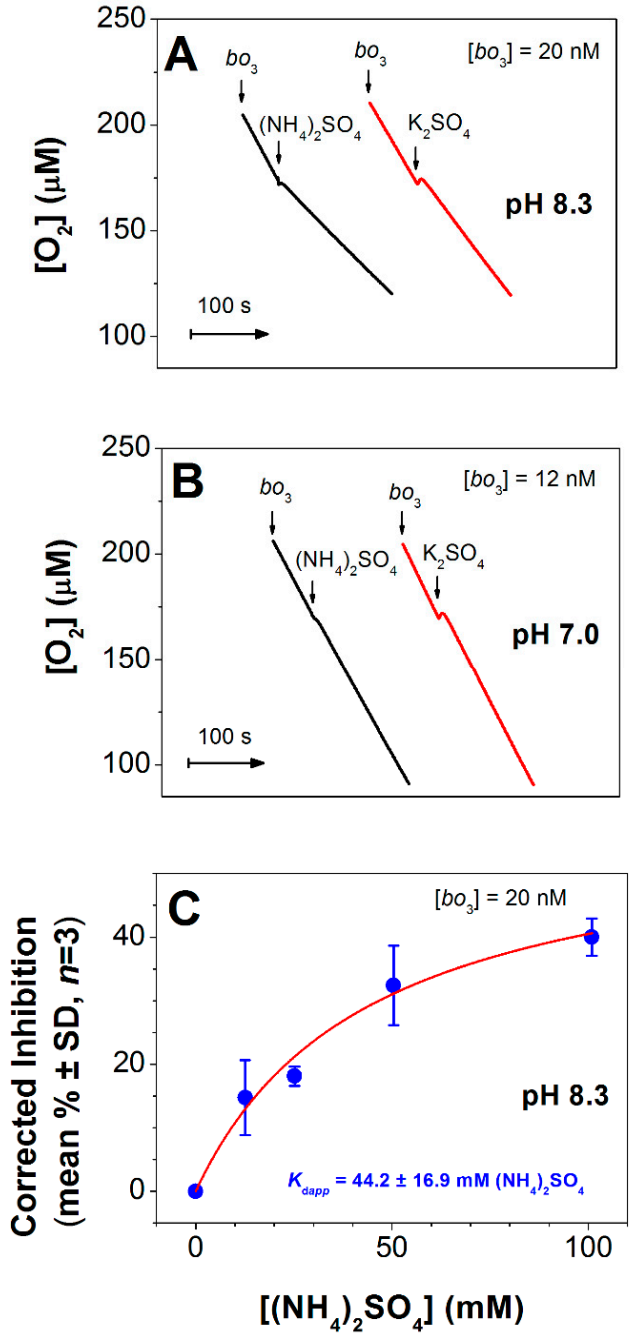

Figure 1. Effect of $(NH_4)_2SO_4$ on cytochrome bo_3 activity. (**A**) O_2 consumption traces at pH 8.3. 50 mM $(NH_4)_2SO_4$ inhibits the enzyme by 51% whereas 50 mM K_2SO_4 inhibits the enzyme by 18% (n = 3 for each experimental condition). (**B**) O_2 consumption traces at pH 7.0. Neither 50 mM $(NH_4)_2SO_4$ nor 50 mM K_2SO_4 affects the oxidase activity. (**C**) Percentage inhibition of O_2 reductase activity of cytochrome bo_3 measured at pH 8.3 at increasing concentration of $(NH_4)_2SO_4$. The effect of increasing ionic strength on enzyme activity is taken into account for each data point by subtracting the percent inhibition value in the presence of K_2SO_4 (control) from that in the presence of $(NH_4)_2SO_4$ at the same concentration. Experimental data (filled circles) are shown together with their best fit (solid line) to the hyperbolic equation (see Materials and Methods), giving a maximum percent inhibition value A_{max} of 58.4 ± 10.1%, and K_{dapp} of 44.2 ± 16.9 mM $(NH_4)_2SO_4$ (8.9 ± 3.4 mM NH_3) (mean ± standard deviation, n = 3, R^2 = 0.83663). O_2 reductase activity of cytochrome bo_3 is sustained by 10 mM DTT and 0.25 mM Q_1. Enzyme, 20 nM (**A**,**C**) or 12 nM (**B**). In the absence of $(NH_4)_2SO_4$, V_{max} values are 28 ± 2 and 60 ± 5 mol O_2/mol enzyme/s at pH 8.3 and 7.0, respectively.

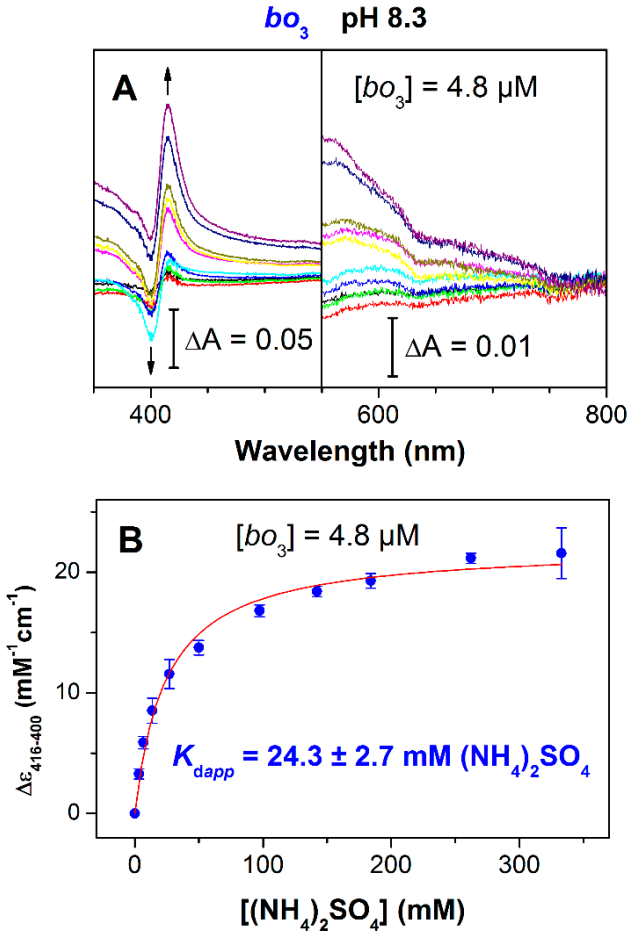

Figure 2. Absorbance changes of oxidized cytochrome bo_3 induced by $(NH_4)_2SO_4$. (**A**) Double difference absorption spectra of the isolated cytochrome bo_3 (4.8 μM): each spectrum is a difference between two difference spectra, $(NH_4)_2SO_4$-treated oxidized minus oxidized and K_2SO_4-treated oxidized minus oxidized at the same concentration of the sulfate. The arrows depict the direction of absorbance changes at increasing $[(NH_4)_2SO_4]$. (**B**) Absorbance changes measured at 416–400 nm as a function of $[(NH_4)_2SO_4]$. Experimental data (*filled circles*) are shown together with their best fit (*solid line*) to the hyperbolic equation (see Materials and Methods), giving the value for maximum absorption change at 416–400 nm A_{max} of 22.1 ± 0.6 $mM^{-1}cm^{-1}$, and K_{dapp} of 24.3 ± 2.7 mM $(NH_4)_2SO_4$ (4.9 ± 0.5 mM NH_3) (mean ± standard deviation, n = 3, R^2 = 0.98947).

3.3. Effect of $(NH_4)_2SO_4$ on O_2 Reductase Activity of E. coli Cytochrome bd-I

Next, we studied the influence $(NH_4)_2SO_4$ on the O_2-reductase activity of the isolated cytochrome *bd*-I from *E. coli* under the same conditions as used for the bo_3 oxidase. We found that in contrast to cytochrome bo_3, cytochrome *bd*-I is not inhibited by millimolar concentrations of $(NH_4)_2SO_4$ at pH 8.3. Furthermore, under these conditions, activation of the catalytic activity of the enzyme was observed.

As shown in Figure 3A, at pH 8.3 the addition of 25 mM $(NH_4)_2SO_4$ increased the rate of O_2 consumption of cytochrome *bd*-I by 39%. In the control with 25 mM K_2SO_4, the increase in the rate was significantly lower (by 11%). At pH 7.0, there was no effect of $(NH_4)_2SO_4$ on the O_2 reductase activity of cytochrome *bd*-I (Figure 3B). At pH 8.3, the O_2 reductase activity of cytochrome *bd*-I increased with an increase in ammonia concentration (Figure 3C). Maximum activation in enzyme activity, 140%, was observed following the addition of 100 mM $(NH_4)_2SO_4$ (after subtraction of the control with K_2SO_4).

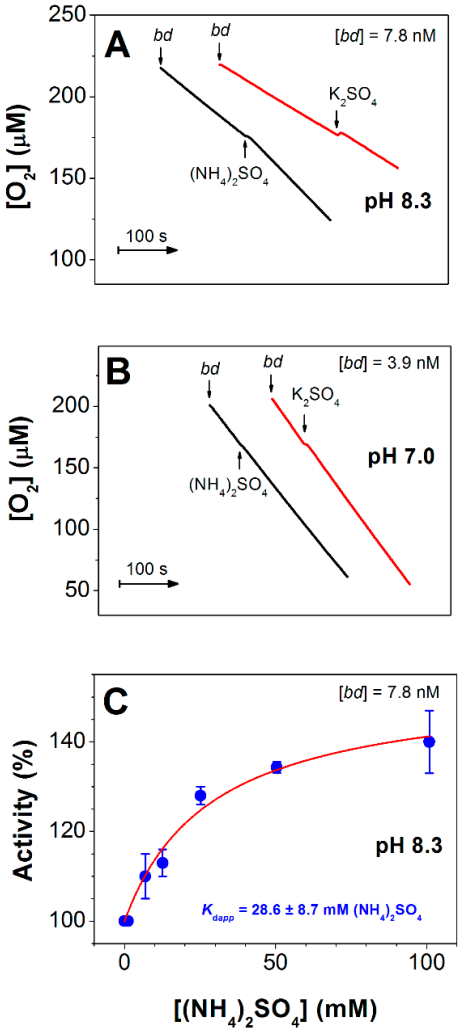

Figure 3. Effect of $(NH_4)_2SO_4$ on cytochrome *bd*-I activity. (**A**) O_2 consumption traces at pH 8.3. A total of 25 mM $(NH_4)_2SO_4$ increases O_2 consumption rate of the enzyme by 39% whereas 25 mM K_2SO_4 increases the rate by 11% (n = 3 for each experimental condition). (**B**) O_2 consumption traces at pH 7.0. Neither 25 mM $(NH_4)_2SO_4$ nor 25 mM K_2SO_4 affects the oxidase activity. (**C**) Dependence of O_2 reductase activity of cytochrome *bd*-I measured at pH 8.3 on the concentration of $(NH_4)_2SO_4$. Values are expressed with reference to the activity measured before sulfate addition taken as 100%. The effect of increasing ionic strength on enzyme activity is taken into account for each data point by subtracting the activity value in the presence of K_2SO_4 (control) from that in the presence of $(NH_4)_2SO_4$ at the same concentration. Experimental data (filled circles) are shown together with their best fit (solid line) to the hyperbolic equation (see Materials and Methods), giving a maximum activity value A_{max} of 152.9 ± 6.3%, and K_{dapp} of 28.6 ± 8.7 mM $(NH_4)_2SO_4$ (5.7 ± 1.7 mM NH_3) (mean ± standard deviation, n = 3, R^2 = 0.92789). O_2 reductase activity of cytochrome *bd*-I is sustained by 10 mM DTT and 0.25 mM Q_1. Enzyme, 7.8 nM (**A**,**C**) or 3.9 nM (**B**). In the absence of $(NH_4)_2SO_4$, V_{max} values are 30 ± 6 and 152 ± 15 mol O_2/mol enzyme/s at pH 8.3 and 7.0, respectively.

We also studied the effect of $(NH_4)_2SO_4$ on O_2 consumption by *E. coli* mutant cells containing cytochrome *bd*-I as the only terminal oxidase. Supplementary Figures S1A and S2 show that at pH 8.3 the addition of $(NH_4)_2SO_4$ up to 27 mM increased respiration of the intact cells. Maximum acceleration of the O_2 consumption rate (140%) was observed at 27 mM $(NH_4)_2SO_4$. In the control with K_2SO_4 added at the same concentrations, there was no significant change in O_2 consumption by the cells.

3.4. Effect of $(NH_4)_2SO_4$ on Absorption Spectra of E. coli Cytochrome bd-I

Finally, we found that ammonia affects the absorption spectrum of the isolated cytochrome *bd*-I in the fully oxidized state. Figure 4A displays the spectral changes caused by the addition of $(NH_4)_2SO_4$ at millimolar concentrations to the oxidized *bd*-I enzyme at pH 8.3.

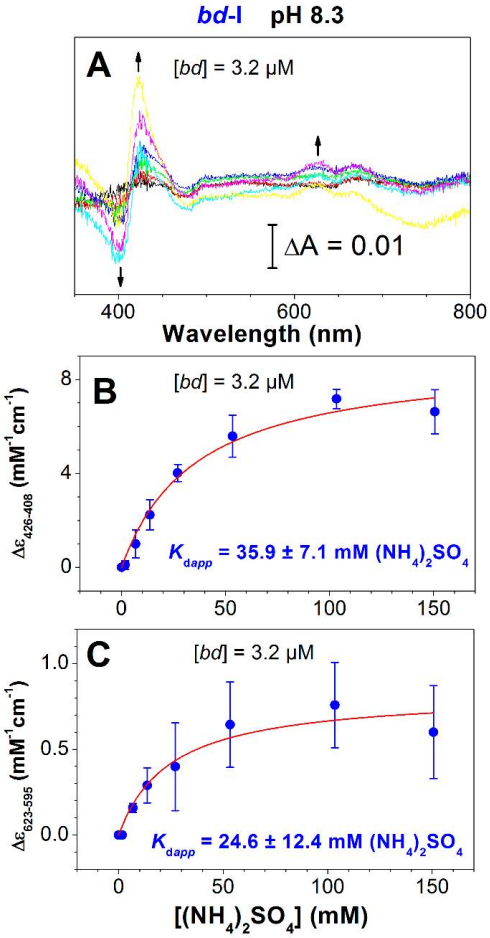

Figure 4. Absorbance changes of oxidized cytochrome *bd*-I induced by $(NH_4)_2SO_4$. (**A**) Double difference absorption spectra of the isolated cytochrome *bd*-I (3.2 μM): each spectrum is a difference between two difference spectra, $(NH_4)_2SO_4$-treated oxidized minus oxidized and K_2SO_4-treated oxidized minus oxidized at the same concentration of the sulfate. The arrows depict the direction of absorbance changes at increasing [$(NH_4)_2SO_4$]. (**B**,**C**) Absorbance changes measured at 426–408 and 623–595 nm as a function of $(NH_4)_2SO_4$. Experimental data (filled circles) are shown together with their best fits (solid lines) to the hyperbolic equation (see Materials and Methods), giving the values for maximum absorption changes at 426–408 and 623–595 nm A_{max} of 8.9 ± 0.6 and 0.8 ± 0.1 mM^{-1}cm^{-1} and K_{dapp} of 35.9 ± 7.1 and 24.6 ± 12.4 mM $(NH_4)_2SO_4$ (7.2 ± 1.4 and 4.9 ± 2.5 mM NH_3), respectively (mean ± standard deviation, n = 3; R^2 = 0.94547 (Soret region), R^2 = 0.69231 (visible region)).

In the Soret region, the ammonia-induced spectrum showed a red shift with a maximum at about 423–428 nm and a minimum around 395–408 nm. In the near-IR region, there were two maxima at ~623 and ~673 nm, and a broad minimum at ~740 nm. The changes may report the interaction of ammonia with the ferric heme *d*. The magnitude of the changes increased with increasing concentrations of $(NH_4)_2SO_4$. Analysis of the absorption titration curves measured at 426–408 and 623–595 nm (Figure 4B,C) yields K_{dapp} of 35.9 ± 7.1 and 24.6 ± 12.4 mM $(NH_4)_2SO_4$, respectively. The titration profile (Figure 4B,C) is similar to that for the plot of percent enzyme activity versus $(NH_4)_2SO_4$ (Figure 3C).

No spectral change was observed, when under the same conditions, $(NH_4)_2SO_4$ was added to cytochrome *bd*-I in the dithionite-reduced state.

4. Discussion

4.1. Proposed Mechanism for Inhibition of Cytochrome bo_3 by Ammonia

The interaction of ammonia with a quinol oxidase has not been investigated before. Recently, von der Hocht et al. observed that in the presence of 20 mM $(NH_4)_2SO_4$ at pH 9 the activity of the isolated aa_3-type cytochrome *c* oxidase from *Paracoccus denitrificans* sustained by ascorbate, *N*,*N*,*N*′,*N*′-tetramethyl-*p*-phenylenediamine and cytochrome *c* decreased by 22% [43]. They also reported that at pH 9 the addition of ammonia to the H_2O_2-generated **F** state led to its conversion into a novel **P** state called $\mathbf{P_N}$ [43]. **P** and **F** are two transient ferryl intermediates formed sequentially during the catalytic cycle of both heme-copper and *bd*-type terminal oxidases [44–50]. In the case of cytochrome *c* oxidase, spectrally similar artificial **P** and **F** intermediates can also be produced by the addition of H_2O_2 at different concentrations to the enzyme in the oxidized (**O**) state at alkaline pH [51,52]. In the new $\mathbf{P_N}$ state [43], ammonia binds to Cu_B, as shown by resonance Raman spectroscopy [53].

Here, we showed that the O_2 consumption of the isolated *E. coli* cytochrome bo_3, sustained by DTT and Q_1, was inhibited by $(NH_4)_2SO_4$ at pH 8.3 (Figure 1A). At the maximum concentration of $(NH_4)_2SO_4$ used (100 mM), the enzyme activity decreased by 40% (Figure 1C). The inhibition was not observed at pH 7.0. The pK_a of ammonium in aqueous solution is known to be 9.25 at 25 °C. Using the Henderson-Hasselbalch equation one can calculate that when 100 mM of $(NH_4)_2SO_4$ is added to the sample at pH 8.3 $[NH_4^+]$ = 179.85 mM and $[NH_3]$ = 20.15 mM, whereas at pH 7.0 $[NH_4^+]$ = 198.88 mM and $[NH_3]$ = 1.12 mM. In other words, by shifting the pH from 7.0 to 8.3, $[NH_3]$ increases 18 times, while $[NH_4^+]$ does not change significantly (decreases only 1.1 times). Thus, we can conclude that it is ammonia rather than the ammonium ion that inhibits cytochrome bo_3.

At pH 8.3, ammonia caused a red shift in the Soret band of the oxidized cytochrome bo_3 (Figure 2A). The magnitude of the absorption changes increased with increasing the ligand concentration giving K_{dapp} of 24.3 ± 2.7 mM $(NH_4)_2SO_4$ that corresponds to 4.9 ± 0.5 mM NH_3 (Figure 2B). The titration profile was similar to that for the inhibition of the enzyme activity by ammonia (Figure 1C). Ingledew et al. earlier reported that the addition of cyanide induces a red shift in the Soret band of the oxidized cytochrome bo_3 [54]. The binding of a ligand to the high-spin heme brings about a red shift of the Soret band in enzyme absorption spectra [1,54,55]. On the contrary, no absorption change or a small blue shift in the Soret band was observed when a ligand binds to Cu_B [1,56]. Thus, we suggest that ammonia binds to heme o_3. This conclusion is supported by the fact that the ligand-induced red shift in the Soret band was accompanied by the loss of the broad charge transfer band around 630 nm (Figure 2A). The 630-nm band is characteristic of the fully oxidized binuclear site in which heme o_3 is in a high-spin state [54]. The decay of this band suggests the conversion of the high-spin heme o_3 into the low-spin ammonia complex. As a ferric heme usually binds an anion, we propose that NH_3 binds to heme o_3 in the form of NH_2^- with the release of H^+. Both cyanide and azide can bridge between the ferric heme o_3 and cupric Cu_B forming the following structures: Fe_{o3}^{3+}–C=N–Cu_B^{2+} and Fe_{o3}^{3+}–N=N=N–Cu_B^{2+}, where Fe_{o3} is the heme o_3 iron [55,57,58]. Compared to these two ligands, ammonia is a much smaller molecule. Rather, NH_3 can be compared to a water/hydroxide molecule that is a natural ligand of Cu_B in several states of the catalytic cycle of heme–copper oxidases [59]. For this reason, NH_3 cannot be a bridging ligand at the binuclear site since a distance is around 4–5 Å. However, the binding of two NH_3 molecules at the oxidized binuclear site at a time, one to heme o_3 and the other to Cu_B, may occur. Indeed, NH_3 is approximately the size of a water/hydroxide molecule. In some catalytic intermediates of a heme–copper oxidase, two molecules of H_2O (or OH^-) can bind simultaneously at the binuclear site [59–61]. It could also be true for ammonia. We propose to designate the ammonia adduct of the oxidized cytochrome bo_3 as **N**.

Importantly, the binding of hydroxide (as opposed to water) with the oxidized heme at the binuclear site leads to the transition of the heme from the high-spin to the low-spin state [62]. This process is enhanced at alkaline pH. For instance, at pH 9, about 50% of the ferric heme a_3 is hydroxide-ligated whereas at pH 6.5, no hydroxide is bound to the heme [63]. The spectral shift caused by ammonia (Figure 2A) is similar to the effect of the formation of low-spin complexes of the initial high-spin heme with anionic ligands at the binuclear site. We suggest that when ammonia binds to the oxidized heme at alkaline pH, the complex with deprotonated ammonia (NH_2^-) is formed, just as it happens with hydroxide. It has to be noted that a similar complex can be produced in cytochrome *c* nitrite reductase, before the release of the neutral ammonia, the final product of nitrite reduction, from the catalytic site [64]. Notably, the presence of a tyrosine residue near the heme is critically important. In cytochrome *c* nitrite reductase, the residue facilitates the transition of the heme from the high-spin to the low-spin state (via the stabilization of the radical form of the bound NH_2^-) and serves as a proton donor/acceptor [64]. Surprisingly, all heme–copper oxidases also contain a conserved tyrosine residue that is part of the binuclear site. The tyrosine is bound to Cu_B through a histidine ligand and is critical for the proton pumping function. At the same time, the structure of cytochrome *bd* that lacks the proton pump shows no tyrosine residue nearby heme *d* (or heme b_{595}) [9,10,65]. This could explain the higher sensitivity of the bo_3 oxidase to the inhibitory effect of ammonia as compared to the *bd* oxidase.

Figure 5 shows a proposed molecular mechanism of inhibition of the catalytic activity of cytochrome bo_3 by ammonia. The ligand binds to the catalytic intermediates **O** and **F** thereby blocking the oxygen reduction reaction cycle of the enzyme.

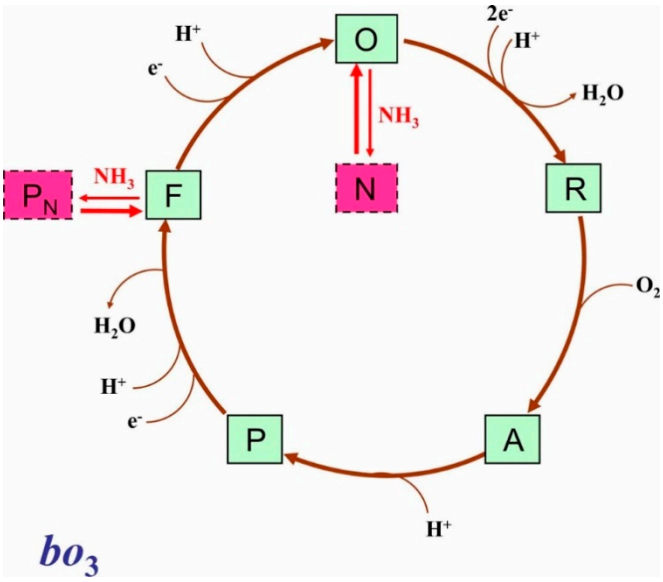

Figure 5. The possible effect of ammonia on the catalytic cycle of cytochrome bo_3. Proposed catalytic intermediates **O** (o_3^{3+}–OH Cu_B^{2+}), **R** (o_3^{2+} Cu_B^{+}), **A** (o_3^{2+}–O_2 Cu_B^{+}), **P** (o_3^{4+}=O^{2-} Cu_B^{2+}–OH), and **F** (o_3^{4+}=O^{2-} Cu_B^{2+}) are shown. Possible redox and ligation state of the binuclear site in each intermediate is indicated in brackets. Only chemical protons are shown. Pumped protons are not shown for clarity. The two ferryl species **P** and **F** likely differ in the presence of an aromatic amino acid radical in **P**, as in the intermediate $\mathbf{P_M}$ of cytochrome *c* oxidase [66]. NH_3 presumably converts **F** into the $\mathbf{P_N}$ state (o_3^{4+}=O^{2-} Cu_B^{2+}–NH_3) and **O** into the ammonia complex **N** (o_3^{3+}–NH_2^- Cu_B^{2+} and/or o_3^{3+}– NH_2^- Cu_B^{2+}–NH_3), thereby leading to the inhibition of the oxidase activity.

4.2. Proposed Mechanism for Ammonia-Induced Acceleration of the Cytochrome bd-I Activity

In contrast to cytochrome bo_3, cytochrome *bd*-I at pH 8.3 was not inhibited by $(NH_4)_2SO_4$ (Figure 3A). Furthermore, the addition of the ligand led to an increase in enzyme activity. The highest enhancement of the rate of cytochrome *bd*-I-catalyzed reaction (140%) was

achieved upon the addition of 100 mM $(NH_4)_2SO_4$ (Figure 3C). The fact that at pH 7.0 $(NH_4)_2SO_4$ did not affect the enzyme activity (Figure 3B) suggests that the activator was ammonia rather than the ammonium ion. Consistently, the addition of $(NH_4)_2SO_4$ to intact cells of the *E. coli* mutant possessing cytochrome *bd*-I as the sole terminal oxidase at pH 8.3 increased cell respiration (Supplementary Figures S1A and S2). Maximum acceleration of the O_2 consumption rate (140%) was observed at 27 mM $(NH_4)_2SO_4$.

At pH 8.3, the addition of ammonia brought about spectral changes in the fully oxidized cytochrome *bd*-I, the amplitude of which increased with increasing the ligand concentration (Figure 4). The titration curves (Figure 4B,C) were similar to that of the ammonia-induced activity change (Figure 3C). Surprisingly, the ammonia-induced difference absorption spectra (Figure 4A) were similar to the difference absorption spectra recorded following addition of H_2O_2 to the fully oxidized cytochrome *bd*-I [67,68]. In the reaction product, heme *d* was in the ferryl state [69]. As in the case of cytochrome *c* oxidase [51,52], after the addition of excess peroxide to cytochrome *bd*-I, the two ferryl species, P and F, were probably produced. P discovered by [47] is a heme *d* ferryl porphyrin π-cation radical intermediate [49]. Thus, the H_2O_2-induced difference spectra reported in [67,68] likely reflect a mixture of P and F.

It is known that in the air-oxidized cytochromes *bd* from *E. coli* and *Azotobacter vinelandii* heme *d* is mostly in the oxygenated form [7,40,70,71]. This state is often called compound A^1 (see Figure 6). Jünemann and Wrigglesworth reported that exposure of the *A. vinelandii* cytochrome *bd* in an air-oxidized state to alkaline pH leads to deoxygenation of heme *d* [71]. At alkaline pH, the heme *d* oxy-complex in the A^1 state is destabilized and may decay to the oxidized (O) state (Figure 6).

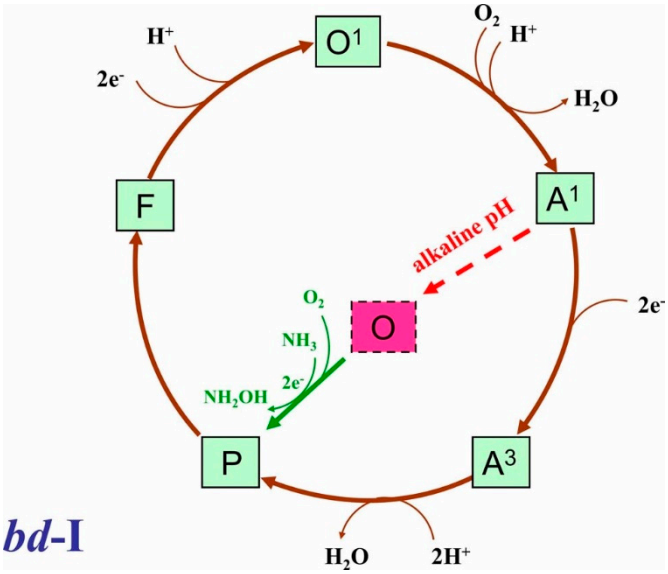

Figure 6. The possible effect of ammonia on the catalytic cycle of cytochrome *bd*-I. Enzyme catalytic intermediates **O**$^{\mathbf{1}}$ ($b_{558}{}^{2+}$ $b_{595}{}^{3+}$ d^{3+}–OH), **A**$^{\mathbf{1}}$ ($b_{558}{}^{3+}$ $b_{595}{}^{3+}$ d^{2+}–O_2), **A**$^{\mathbf{3}}$ ($b_{558}{}^{2+}$ $b_{595}{}^{2+}$ d^{2+}–O_2), **P** ($b_{558}{}^{2+}$ $b_{595}{}^{3+}$ d^{*4+}=O^2 where d^{*4+}=O^2 is a ferryl porphyrin π-cation radical [47,49]), and **F** ($b_{558}{}^{3+}$ $b_{595}{}^{3+}$ d^{4+}=O^{2-}) are shown. At alkaline pH, **A**$^{\mathbf{1}}$ is probably converted into the fully oxidized form **O**. **O** is not involved in the catalytic cycle [72]. NH_3 possibly promotes the formation of **P** from **O**, thereby leading to the acceleration of the oxidase activity. It is also possible that NH_3 reacts with **O**$^{\mathbf{1}}$ producing **F**. In the latter two reactions, NH_3 serves as a two-electron donor being oxidized to NH_2OH. The reaction of NH_3 with **O**$^{\mathbf{1}}$ is not shown for the sake of simplicity.

A^1 is a catalytic intermediate of cytochrome *bd*-I [73], whereas O does not participate in the catalytic cycle [72]. The conversion of A^1 into O under alkaline conditions seems to correlate with the observation that the O_2-reductase activity of cytochrome *bd*-I at pH 8.3 is lower than that at pH 7.0 (V_{max} of 30 ± 6 mol O_2/mol enzyme/s at pH 8.3 versus

152 ± 15 mol O_2/mol enzyme/s at pH 7.0). We hypothesize that the addition of ammonia to the oxidized cytochrome *bd*-I at pH 8.3 promotes the formation of P from O (Figure 6), thereby increasing the enzyme activity. NH_3 may be oxidized to NH_2OH serving as a two-electron donor in this reaction. NH_3 could also react with the one electron-reduced enzyme (O^1) with the production of F and NH_2OH.

4.3. Possible Physiological Significance of the Difference between Cytochrome bo_3 and Cytochrome bd-I in Sensitivity toward Ammonia for E. coli

Along with nitric oxide, carbon monoxide, and hydrogen sulfide, ammonia is considered as a "gasotransmitter" or endogenously generated gaseous signaling molecule [74]. A signaling role of NH_3 in cultured rat astrocytes has been reported [75]. The molecule can move across the plasma membranes both passively [76] and actively via the Amt/Rh family of ammonium/ammonia transporting membrane proteins, involving the electrogenic transport mechanism [77,78]. Ammonia is a degradation product of proteins, peptides, amino acids, and urea. It is mainly produced by the gut microbiota and the gut, liver, kidney, and muscle cells. An adult human gut generates 4–10 g of NH_3 daily [79]. *E. coli* is one of the most active ammonia-producers in the gut microbiota. Ammonia can also be recycled into amino acid synthesis [80]. NH_3 is a potent infochemical in bacteria–bacteria interactions. It is able to induce oxidative stress responses and increase resistance to antibiotics thus playing a role in defense mechanisms against antimicrobials [81]. At high enough concentrations, ammonia is toxic to cells, especially to neurons. For this reason, the plasma concentration of ammonia in healthy adults is maintained in the range of 10–35 μM [82]. In the intestines, the total ammonia concentration depends on intestinal segment and diet but in general it is about 1000-times higher than in blood [34]. The highest ammonia concentration in the body (27.2 ± 17.5 mM) is reported to be in the large intestinal lumen [34]. Intestinal pH shows high variability depending on the intestinal segment, diet, and regional distribution of microbiota, and there are conditions in which the pH values are in the alkaline region [83,84]. For example, in the distal ileum, the median pH is 8.1 [85]. In light of the above, we suggest that the difference between the two quinol oxidases in the sensitivity toward ammonia can have a physiological significance for *E. coli* and other enterobacteria. In contrast to the heme–copper oxidase bo_3 that is inhibited by NH_3 at alkaline pH, the *bd*-I oxidase under the same conditions is not inhibited but activated by the ligand. Thus cytochrome *bd* can sustain bacterial respiration in the presence of high concentrations of not only sulfide [26,27,86], but also ammonia.

5. Conclusions

In summary, we investigated the sensitivity of two physiologically important respiratory cytochromes of *E. coli*, bo_3 and *bd*-I, to ammonia at the level of both isolated enzymes and intact cells. It turned out that at pH 8.3 the isolated heme-copper bo_3 oxidase is partly inhibited by NH_3. Surprisingly, under the same conditions, the isolated copper-lacking *bd*-I enzyme is not only resistant to but also activated by this gaseous signaling molecule. Consistently, respiration of intact cells of the *E. coli* mutant that relies on cytochrome *bd*-I as the only terminal oxidase is accelerated by NH_3. With such a unique trait, the *bd*-type redox enzyme may provide *E. coli* and perhaps other bacteria with the ability to maintain the aerobic energy metabolism in the gut and other ammonia-rich environments.

Supplementary Materials: The following are available online at https://www.mdpi.com/2076-3921/10/1/13/s1, Figure S1: O_2 consumption traces showing the effect of $(NH_4)_2SO_4$ on the respiration of *E. coli* in respiratory mutants at pH 8.3, Figure S2: Effect of $(NH_4)_2SO_4$ on the respiration of *E. coli* in respiratory mutants.

Author Contributions: Conceptualization, E.F. and V.B.B.; methodology, E.F., S.A.S. and V.B.B.; formal analysis, V.B.B.; investigation, E.F. and V.B.B.; data curation, E.F. and V.B.B.; writing—original draft preparation, E.F., S.A.S. and V.B.B.; writing—review and editing, E.F., S.A.S. and V.B.B.; visualization, E.F., S.A.S. and V.B.B.; funding acquisition, E.F. and V.B.B. All authors have read and agreed to the published version of the manuscript.

Funding: This research was funded by the Russian Foundation for Basic Research (http://www.rfbr.ru/rffi/eng)—research project number 19-04-00094 (to V.B.B.) and by Sapienza grant number RP1181643681A66B (to E.F.).

Acknowledgments: The authors are indebted to Robert Gennis (University of Illinois at Urbana-Champaign) for the *E. coli* strain GO105/pTK1, Alex Ter Beek and Joost Teixeira de Mattos (University of Amsterdam) for the *E. coli* strains TBE025 and TBE037, and Marina Verkhovskaya (University of Helsinki) for the purified *E. coli* cytochrome bo_3. The authors thank Maria Petrosino, Martina Roberta Nastasi and Francesca Giordano for their help with the *E. coli* cell experiments.

Conflicts of Interest: The authors declare no conflict of interest. The funders had no role in the design of the study; in the collection, analyses, or interpretation of data; in the writing of the manuscript, or in the decision to publish the results.

Abbreviations

K_{dapp}	Apparent dissociation constant
DTT	Dithiothreitol
Q_1	2,3-dimethoxy-5-methyl-6-(3-methyl-2-butenyl)-1,4-benzoquinone

References

1. Borisov, V.B.; Verkhovsky, M.I. Oxygen as Acceptor. *EcoSal Plus* **2015**, *6*. [CrossRef] [PubMed]
2. Melo, A.M.; Teixeira, M. Supramolecular organization of bacterial aerobic respiratory chains: From cells and back. *Biochim. Biophys. Acta* **2016**, *1857*, 190–197. [CrossRef] [PubMed]
3. Borisov, V.B.; Gennis, R.B.; Hemp, J.; Verkhovsky, M.I. The cytochrome *bd* respiratory oxygen reductases. *Biochim. Biophys. Acta* **2011**, *1807*, 1398–1413. [CrossRef] [PubMed]
4. Puustinen, A.; Finel, M.; Haltia, T.; Gennis, R.B.; Wikstrom, M. Properties of the two terminal oxidases of *Escherichia coli*. *Biochemistry* **1991**, *30*, 3936–3942. [CrossRef] [PubMed]
5. Jasaitis, A.; Borisov, V.B.; Belevich, N.P.; Morgan, J.E.; Konstantinov, A.A.; Verkhovsky, M.I. Electrogenic reactions of cytochrome *bd*. *Biochemistry* **2000**, *39*, 13800–13809. [CrossRef]
6. Belevich, I.; Borisov, V.B.; Zhang, J.; Yang, K.; Konstantinov, A.A.; Gennis, R.B.; Verkhovsky, M.I. Time-resolved electrometric and optical studies on cytochrome *bd* suggest a mechanism of electron-proton coupling in the di-heme active site. *Proc. Natl. Acad. Sci. USA* **2005**, *102*, 3657–3662. [CrossRef]
7. Borisov, V.B.; Murali, R.; Verkhovskaya, M.L.; Bloch, D.A.; Han, H.; Gennis, R.B.; Verkhovsky, M.I. Aerobic respiratory chain of *Escherichia coli* is not allowed to work in fully uncoupled mode. *Proc. Natl. Acad. Sci. USA* **2011**, *108*, 17320–17324. [CrossRef]
8. Abramson, J.; Riistama, S.; Larsson, G.; Jasaitis, A.; Svensson-Ek, M.; Laakkonen, L.; Puustinen, A.; Iwata, S.; Wikstrom, M. The structure of the ubiquinol oxidase from *Escherichia coli* and its ubiquinone binding site. *Nat. Struct. Biol.* **2000**, *7*, 910–917. [CrossRef]
9. Safarian, S.; Hahn, A.; Mills, D.J.; Radloff, M.; Eisinger, M.L.; Nikolaev, A.; Meier-Credo, J.; Melin, F.; Miyoshi, H.; Gennis, R.B.; et al. Active site rearrangement and structural divergence in prokaryotic respiratory oxidases. *Science* **2019**, *366*, 100–104. [CrossRef]
10. Theßeling, A.; Rasmussen, T.; Burschel, S.; Wohlwend, D.; Kagi, J.; Muller, R.; Bottcher, B.; Friedrich, T. Homologous *bd* oxidases share the same architecture but differ in mechanism. *Nat. Commun.* **2019**, *10*, 5138. [CrossRef]
11. Pereira, M.M.; Santana, M.; Teixeira, M. A novel scenario for the evolution of haem-copper oxygen reductases. *Biochim. Biophys. Acta* **2001**, *1505*, 185–208. [CrossRef]
12. Capitanio, N.; Palese, L.L.; Capitanio, G.; Martino, P.L.; Richter, O.M.; Ludwig, B.; Papa, S. Allosteric interactions and proton conducting pathways in proton pumping aa_3 oxidases: Heme *a* as a key coupling element. *Biochim. Biophys. Acta* **2012**, *1817*, 558–566. [CrossRef] [PubMed]
13. Maneg, O.; Malatesta, F.; Ludwig, B.; Drosou, V. Interaction of cytochrome *c* with cytochrome oxidase: Two different docking scenarios. *Biochim. Biophys. Acta* **2004**, *1655*, 274–281. [CrossRef] [PubMed]
14. Borisov, V.B.; Siletsky, S.A. Features of organization and mechanism of catalysis of two families of terminal oxidases: Heme-copper and *bd*-type. *Biochemistry (Mosc)* **2019**, *84*, 1390–1402. [CrossRef] [PubMed]
15. Siletsky, S.A.; Borisov, V.B.; Mamedov, M.D. Photosystem II and terminal respiratory oxidases: Molecular machines operating in opposite directions. *Front. Biosci. (Landmark Ed.)* **2017**, *22*, 1379–1426. [CrossRef]
16. Forte, E.; Giuffre, A.; Huang, L.S.; Berry, E.A.; Borisov, V.B. Nitric oxide does not inhibit but is metabolized by the cytochrome *bcc-aa*$_3$ supercomplex. *Int. J. Mol. Sci.* **2020**, *21*, 8521. [CrossRef]
17. Choi, S.K.; Schurig-Briccio, L.; Ding, Z.; Hong, S.; Sun, C.; Gennis, R.B. Location of the substrate binding site of the cytochrome bo_3 ubiquinol oxidase from *Escherichia coli*. *J. Am. Chem. Soc.* **2017**, *139*, 8346–8354. [CrossRef]
18. Arutyunyan, A.M.; Sakamoto, J.; Inadome, M.; Kabashima, Y.; Borisov, V.B. Optical and magneto-optical activity of cytochrome *bd* from *Geobacillus thermodenitrificans*. *Biochim. Biophys. Acta* **2012**, *1817*, 2087–2094. [CrossRef]

19. Cotter, P.A.; Chepuri, V.; Gennis, R.B.; Gunsalus, R.P. Cytochrome *o* (*cyoABCDE*) and *d* (*cydAB*) oxidase gene expression in *Escherichia coli* is regulated by oxygen, pH, and the *fnr* gene product. *J. Bacteriol.* **1990**, *172*, 6333–6338. [CrossRef]
20. D'Mello, R.; Hill, S.; Poole, R.K. The oxygen affinity of cytochrome *bo*' in *Escherichia coli* determined by the deoxygenation of oxyleghemoglobin and oxymyoglobin: K_m values for oxygen are in the submicromolar range. *J. Bacteriol.* **1995**, *177*, 867–870. [CrossRef]
21. Belevich, I.; Borisov, V.B.; Konstantinov, A.A.; Verkhovsky, M.I. Oxygenated complex of cytochrome *bd* from *Escherichia coli*: Stability and photolability. *FEBS Lett.* **2005**, *579*, 4567–4570. [CrossRef] [PubMed]
22. Borisov, V.B.; Forte, E.; Konstantinov, A.A.; Poole, R.K.; Sarti, P.; Giuffre, A. Interaction of the bacterial terminal oxidase cytochrome *bd* with nitric oxide. *FEBS Lett.* **2004**, *576*, 201–204. [CrossRef]
23. Borisov, V.B.; Forte, E.; Sarti, P.; Brunori, M.; Konstantinov, A.A.; Giuffre, A. Redox control of fast ligand dissociation from *Escherichia coli* cytochrome *bd*. *Biochem. Biophys. Res. Commun.* **2007**, *355*, 97–102. [CrossRef] [PubMed]
24. Mason, M.G.; Shepherd, M.; Nicholls, P.; Dobbin, P.S.; Dodsworth, K.S.; Poole, R.K.; Cooper, C.E. Cytochrome *bd* confers nitric oxide resistance to *Escherichia coli*. *Nat. Chem. Biol.* **2009**, *5*, 94–96. [CrossRef] [PubMed]
25. Shepherd, M.; Achard, M.E.; Idris, A.; Totsika, M.; Phan, M.D.; Peters, K.M.; Sarkar, S.; Ribeiro, C.A.; Holyoake, L.V.; Ladakis, D.; et al. The cytochrome *bd*-I respiratory oxidase augments survival of multidrug-resistant *Escherichia coli* during infection. *Sci. Rep.* **2016**, *6*, 35285. [CrossRef] [PubMed]
26. Forte, E.; Borisov, V.B.; Falabella, M.; Colaco, H.G.; Tinajero-Trejo, M.; Poole, R.K.; Vicente, J.B.; Sarti, P.; Giuffre, A. The terminal oxidase cytochrome *bd* promotes sulfide-resistant bacterial respiration and growth. *Sci. Rep.* **2016**, *6*, 23788. [CrossRef] [PubMed]
27. Korshunov, S.; Imlay, K.R.; Imlay, J.A. The cytochrome *bd* oxidase of *Escherichia coli* prevents respiratory inhibition by endogenous and exogenous hydrogen sulfide. *Mol. Microbiol.* **2016**, *101*, 62–77. [CrossRef] [PubMed]
28. Forte, E.; Borisov, V.B.; Siletsky, S.A.; Petrosino, M.; Giuffre, A. In the respiratory chain of *Escherichia coli* cytochromes *bd*-I and *bd*-II are more sensitive to carbon monoxide inhibition than cytochrome bo_3. *Biochim. Biophys. Acta Bioenerg.* **2019**, *1860*, 148088. [CrossRef]
29. Borisov, V.B.; Forte, E.; Siletsky, S.A.; Sarti, P.; Giuffre, A. Cytochrome *bd* from *Escherichia coli* catalyzes peroxynitrite decomposition. *Biochim. Biophys. Acta* **2015**, *1847*, 182–188. [CrossRef]
30. Borisov, V.B.; Davletshin, A.I.; Konstantinov, A.A. Peroxidase activity of cytochrome *bd* from *Escherichia coli*. *Biochemistry (Mosc)* **2010**, *75*, 428–436. [CrossRef]
31. Borisov, V.B.; Forte, E.; Davletshin, A.; Mastronicola, D.; Sarti, P.; Giuffre, A. Cytochrome *bd* oxidase from *Escherichia coli* displays high catalase activity: An additional defense against oxidative stress. *FEBS Lett.* **2013**, *587*, 2214–2218. [CrossRef] [PubMed]
32. Al-Attar, S.; Yu, Y.; Pinkse, M.; Hoeser, J.; Friedrich, T.; Bald, D.; de Vries, S. Cytochrome *bd* displays significant quinol peroxidase activity. *Sci. Rep.* **2016**, *6*, 27631. [CrossRef] [PubMed]
33. Borisov, V.B.; Siletsky, S.A.; Paiardini, A.; Hoogewijs, D.; Forte, E.; Giuffre, A.; Poole, R.K. Bacterial oxidases of the cytochrome *bd* family: Redox enzymes of unique structure, function and utility as drug targets. *Antioxid. Redox Signal.* **2020**. [CrossRef] [PubMed]
34. Eklou-Lawson, M.; Bernard, F.; Neveux, N.; Chaumontet, C.; Bos, C.; Davila-Gay, A.M.; Tome, D.; Cynober, L.; Blachier, F. Colonic luminal ammonia and portal blood L-glutamine and L-arginine concentrations: A possible link between colon mucosa and liver ureagenesis. *Amino Acids* **2009**, *37*, 751–760. [CrossRef]
35. Miller, M.J.; Gennis, R.B. The purification and characterization of the cytochrome *d* terminal oxidase complex of the *Escherichia coli* aerobic respiratory chain. *J. Biol. Chem.* **1983**, *258*, 9159–9165.
36. Borisov, V.B. Interaction of *bd*-type quinol oxidase from *Escherichia coli* and carbon monoxide: Heme *d* binds CO with high affinity. *Biochemistry (Mosc)* **2008**, *73*, 14–22. [CrossRef]
37. Puustinen, A.; Verkhovsky, M.I.; Morgan, J.E.; Belevich, N.P.; Wikstrom, M. Reaction of the Escherichia coli quinol oxidase cytochrome bo3 with dioxygen: The role of a bound ubiquinone molecule. *Proc. Natl. Acad. Sci. USA* **1996**, *93*, 1545–1548. [CrossRef]
38. Borisov, V.; Arutyunyan, A.M.; Osborne, J.P.; Gennis, R.B.; Konstantinov, A.A. Magnetic circular dichroism used to examine the interaction of *Escherichia coli* cytochrome *bd* with ligands. *Biochemistry* **1999**, *38*, 740–750. [CrossRef]
39. Cheesman, M.R.; Watmough, N.J.; Pires, C.A.; Turner, R.; Brittain, T.; Gennis, R.B.; Greenwood, C.; Thomson, A.J. Cytochrome *bo* from *Escherichia coli*: Identification of haem ligands and reaction of the reduced enzyme with carbon monoxide. *Biochem. J.* **1993**, *289*, 709–718. [CrossRef]
40. Borisov, V.B.; Smirnova, I.A.; Krasnosel'skaya, I.A.; Konstantinov, A.A. Oxygenated cytochrome *bd* from *Escherichia coli* could be transformed into an oxidized form by lipophilic electron acceptors. *Biokhimiia* **1994**, *59*, 598–606.
41. Eun, H.-M. *Enzymes and Nucleic Acids. Enzymology Primer for Recombinant DNA Technology*; Academic Press: Cambridge, MA, USA, 1996; pp. 1–108. [CrossRef]
42. Puustinen, A.; Morgan, J.E.; Verkhovsky, M.; Thomas, J.W.; Gennis, R.B.; Wikstrom, M. The low spin heme site of cytochrome *o* from *E. coli* is promiscuous with respect to heme type. *Biochemistry* **1992**, *31*, 10363–10369. [CrossRef] [PubMed]
43. Von der Hocht, I.; van Wonderen, J.H.; Hilbers, F.; Angerer, H.; MacMillan, F.; Michel, H. Interconversions of P and F intermediates of cytochrome *c* oxidase from *Paracoccus denitrificans*. *Proc. Natl. Acad. Sci. USA* **2011**, *108*, 3964–3969. [CrossRef] [PubMed]
44. Pinakoulaki, E.; Pfitzner, U.; Ludwig, B.; Varotsis, C. Direct detection of Fe(IV)=O intermediates in the cytochrome aa_3 oxidase from *Paracoccus denitrificans*/H_2O_2 reaction. *J. Biol. Chem.* **2003**, *278*, 18761–18766. [CrossRef] [PubMed]

45. Siletsky, S.A.; Konstantinov, A.A. Cytochrome *c* oxidase: Charge translocation coupled to single-electron partial steps of the catalytic cycle. *Biochim. Biophys. Acta* **2012**, *1817*, 476–488. [CrossRef] [PubMed]
46. Papa, S.; Capitanio, G.; Papa, F. The mechanism of coupling between oxido-reduction and proton translocation in respiratory chain enzymes. *Biol. Rev. Camb. Philos. Soc.* **2018**, *93*, 322–349. [CrossRef]
47. Belevich, I.; Borisov, V.B.; Verkhovsky, M.I. Discovery of the true peroxy intermediate in the catalytic cycle of terminal oxidases by real-time measurement. *J. Biol. Chem.* **2007**, *282*, 28514–28519. [CrossRef]
48. Borisov, V.B.; Belevich, I.; Bloch, D.A.; Mogi, T.; Verkhovsky, M.I. Glutamate 107 in subunit I of cytochrome *bd* from *Escherichia coli* is part of a transmembrane intraprotein pathway conducting protons from the cytoplasm to the heme b_{595}/heme *d* active site. *Biochemistry* **2008**, *47*, 7907–7914. [CrossRef]
49. Paulus, A.; Rossius, S.G.; Dijk, M.; de Vries, S. Oxoferryl-porphyrin radical catalytic intermediate in cytochrome *bd* oxidases protects cells from formation of reactive oxygen species. *J. Biol. Chem.* **2012**, *287*, 8830–8838. [CrossRef]
50. Siletsky, S.A. Steps of the coupled charge translocation in the catalytic cycle of cytochrome *c* oxidase. *Front. Biosci.* **2013**, *18*, 36–57. [CrossRef]
51. Wrigglesworth, J. Formation and reduction of a 'peroxy' intermediate of cytochrome *c* oxidase by hydrogen peroxide. *Biochem. J.* **1984**, *217*, 715–719. [CrossRef]
52. Fabian, M.; Palmer, G. The interaction of cytochrome oxidase with hydrogen peroxide: The relationship of compounds P and F. *Biochemistry* **1995**, *34*, 13802–13810. [CrossRef] [PubMed]
53. Kozuch, J.; von der Hocht, I.; Hilbers, F.; Michel, H.; Weidinger, I.M. Resonance Raman characterization of the ammonia-generated oxo intermediate of cytochrome *c* oxidase from *Paracoccus denitrificans*. *Biochemistry* **2013**, *52*, 6197–6202. [CrossRef] [PubMed]
54. Ingledew, W.J.; Horrocks, J.; Salerno, J.C. Ligand binding to the haem-copper binuclear catalytic site of cytochrome *bo*, a respiratory quinol oxidase from *Escherichia coli*. *Eur. J. Biochem.* **1993**, *212*, 657–664. [CrossRef] [PubMed]
55. Cheesman, M.R.; Watmough, N.J.; Gennis, R.B.; Greenwood, C.; Thomson, A.J. Magnetic-circular-dichroism studies of *Escherichia coli* cytochrome *bo*. Identification of high-spin ferric, low-spin ferric and ferryl [Fe(IV)] forms of heme *o*. *Eur. J. Biochem.* **1994**, *219*, 595–602. [CrossRef] [PubMed]
56. Wever, R.; Muijsers, A.O.; van Gelder, B.F.; Bakker, E.P.; van Buuren, K.J. Biochemical and biophysical studies on cytochrome *c* oxidase. XI. Reaction with azide. *Biochim. Biophys. Acta* **1973**, *325*, 1–7. [CrossRef]
57. Tsubaki, M.; Mogi, T.; Hori, H.; Sato-Watanabe, M.; Anraku, Y. Infrared and EPR studies on cyanide binding to the heme-copper binuclear center of cytochrome *bo*-type ubiquinol oxidase from *Escherichia coli*. Release of a Cu_B-cyano complex in the partially reduced state. *J. Biol. Chem.* **1996**, *271*, 4017–4022. [CrossRef]
58. Tsubaki, M.; Mogi, T.; Hori, H. Fourier-transform infrared studies on azide-binding to the binuclear center of the *Escherichia coli* *bo*-type ubiquinol oxidase. *FEBS Lett.* **1999**, *449*, 191–195. [CrossRef]
59. Siletsky, S.A.; Belevich, I.; Jasaitis, A.; Konstantinov, A.A.; Wikstrom, M.; Soulimane, T.; Verkhovsky, M.I. Time-resolved single-turnover of ba_3 oxidase from *Thermus thermophilus*. *Biochim. Biophys. Acta* **2007**, *1767*, 1383–1392. [CrossRef]
60. Kaila, V.R.; Johansson, M.P.; Sundholm, D.; Laakkonen, L.; Wistrom, M. The chemistry of the Cu_B site in cytochrome *c* oxidase and the importance of its unique His-Tyr bond. *Biochim. Biophys. Acta* **2009**, *1787*, 221–233. [CrossRef]
61. Lucas, M.F.; Rousseau, D.L.; Guallar, V. Electron transfer pathways in cytochrome *c* oxidase. *Biochim. Biophys. Acta* **2011**, *1807*, 1305–1313. [CrossRef]
62. Lanne, B.; Malmstrom, B.G.; Vanngard, T. The influence of pH on the EPR and redox properties of cytochrome *c* oxidase in detergent solution and in phospholipid vesicles. *Biochim. Biophys. Acta* **1979**, *545*, 205–214. [CrossRef]
63. Branden, M.; Namslauer, A.; Hansson, O.; Aasa, R.; Brzezinski, P. Water-hydroxide exchange reactions at the catalytic site of heme-copper oxidases. *Biochemistry* **2003**, *42*, 13178–13184. [CrossRef] [PubMed]
64. Bykov, D.; Plog, M.; Neese, F. Heme-bound nitroxyl, hydroxylamine, and ammonia ligands as intermediates in the reaction cycle of cytochrome c nitrite reductase: A theoretical study. *J. Biol. Inorg. Chem.* **2014**, *19*, 97–112. [CrossRef]
65. Safarian, S.; Rajendran, C.; Muller, H.; Preu, J.; Langer, J.D.; Ovchinnikov, S.; Hirose, T.; Kusumoto, T.; Sakamoto, J.; Michel, H. Structure of a bd oxidase indicates similar mechanisms for membrane-integrated oxygen reductases. *Science* **2016**, *352*, 583–586. [CrossRef] [PubMed]
66. Proshlyakov, D.A.; Pressler, M.A.; DeMaso, C.; Leykam, J.F.; DeWitt, D.L.; Babcock, G.T. Oxygen activation and reduction in respiration: Involvement of redox-active tyrosine 244. *Science* **2000**, *290*, 1588–1591. [CrossRef]
67. Borisov, V.; Gennis, R.; Konstantinov, A.A. Peroxide complex of cytochrome *bd*: Kinetics of generation and stability. *Biochem. Mol. Biol. Int.* **1995**, *37*, 975–982.
68. Borisov, V.B.; Gennis, R.B.; Konstantinov, A.A. Interaction of cytochrome *bd* from *Escherichia coli* with hydrogen peroxide. *Biokhimiia* **1995**, *60*, 315–327.
69. Kahlow, M.A.; Zuberi, T.M.; Gennis, R.B.; Loehr, T.M. Identification of a ferryl intermediate of *Escherichia coli* cytochrome *d* terminal oxidase by Resonance Raman spectrosopy. *Biochemistry* **1991**, *30*, 11485–11489. [CrossRef]
70. Kahlow, M.A.; Loehr, T.M.; Zuberi, T.M.; Gennis, R.B. The oxygenated complex of cytochrome *d* terminal oxidase: Direct evidence for Fe-O_2 coordination in a chlorin-containing enzyme by Resonance Raman spectroscopy. *J. Am. Chem. Soc.* **1993**, *115*, 5845–5846. [CrossRef]
71. Junemann, S.; Wrigglesworth, J.M. Cytochrome *bd* oxidase from *Azotobacter vinelandii*. Purification and quantitation of ligand binding to the oxygen reduction site. *J. Biol. Chem.* **1995**, *270*, 16213–16220. [CrossRef]

72. Yang, K.; Borisov, V.B.; Konstantinov, A.A.; Gennis, R.B. The fully oxidized form of the cytochrome *bd* quinol oxidase from *E. coli* does not participate in the catalytic cycle: Direct evidence from rapid kinetics studies. *FEBS Lett.* **2008**, *582*, 3705–3709. [CrossRef]
73. Borisov, V.B.; Forte, E.; Sarti, P.; Giuffre, A. Catalytic intermediates of cytochrome *bd* terminal oxidase at steady-state: Ferryl and oxy-ferrous species dominate. *Biochim. Biophys. Acta* **2011**, *1807*, 503–509. [CrossRef] [PubMed]
74. Wang, R. Gasotransmitters: Growing pains and joys. *Trends Biochem. Sci.* **2014**, *39*, 227–232. [CrossRef] [PubMed]
75. Karababa, A.; Gorg, B.; Schliess, F.; Haussinger, D. *O*-GlcNAcylation as a novel ammonia-induced posttranslational protein modification in cultured rat astrocytes. *Metab. Brain Dis.* **2014**, *29*, 975–982. [CrossRef] [PubMed]
76. Cueto-Rojas, H.F.; Milne, N.; van Helmond, W.; Pieterse, M.M.; van Maris, A.J.A.; Daran, J.M.; Wahl, S.A. Membrane potential independent transport of NH_3 in the absence of ammonium permeases in *Saccharomyces cerevisiae*. *BMC Syst. Biol.* **2017**, *11*, 49. [CrossRef]
77. Ullmann, R.T.; Andrade, S.L.; Ullmann, G.M. Thermodynamics of transport through the ammonium transporter Amt-1 investigated with free energy calculations. *J. Phys. Chem. B* **2012**, *116*, 9690–9703. [CrossRef]
78. Wacker, T.; Garcia-Celma, J.J.; Lewe, P.; Andrade, S.L. Direct observation of electrogenic NH_4^+ transport in ammonium transport (Amt) proteins. *Proc. Natl. Acad. Sci. USA* **2014**, *111*, 9995–10000. [CrossRef]
79. Oleskin, A.V.; Shenderov, B.A. Neuromodulatory effects and targets of the SCFAs and gasotransmitters produced by the human symbiotic microbiota. *Microb. Ecol. Health Dis.* **2016**, *27*, 30971. [CrossRef]
80. Spinelli, J.B.; Yoon, H.; Ringel, A.E.; Jeanfavre, S.; Clish, C.B.; Haigis, M.C. Metabolic recycling of ammonia via glutamate dehydrogenase supports breast cancer biomass. *Science* **2017**, *358*, 941–946. [CrossRef]
81. Bernier, S.P.; Letoffe, S.; Delepierre, M.; Ghigo, J.M. Biogenic ammonia modifies antibiotic resistance at a distance in physically separated bacteria. *Mol. Microbiol.* **2011**, *81*, 705–716. [CrossRef]
82. Tiso, M.; Schechter, A.N. Nitrate reduction to nitrite, nitric oxide and ammonia by gut bacteria under physiological conditions. *PLoS ONE* **2015**, *10*, e0119712. [CrossRef]
83. Jones, J.H. The relation of the pH of intestinal contents to calcium and phosphorus utilization. *J. Biol. Chem.* **1942**, *142*, 557–567.
84. Koziolek, M.; Grimm, M.; Becker, D.; Iordanov, V.; Zou, H.; Shimizu, J.; Wanke, C.; Garbacz, G.; Weitschies, W. Investigation of pH and temperature profiles in the GI tract of fasted human subjects using the Intellicap((R)) system. *J. Pharm. Sci.* **2015**, *104*, 2855–2863. [CrossRef] [PubMed]
85. Vertzoni, M.; Augustijns, P.; Grimm, M.; Koziolek, M.; Lemmens, G.; Parrott, N.; Pentafragka, C.; Reppas, C.; Rubbens, J.; Van Den Alphabeele, J.; et al. Impact of regional differences along the gastrointestinal tract of healthy adults on oral drug absorption: An UNGAP review. *Eur. J. Pharm. Sci.* **2019**, *134*, 153–175. [CrossRef] [PubMed]
86. Forte, E.; Giuffrè, A. How bacteria breathe in hydrogen sulfide-rich environments. *Biochemist (Lond)* **2016**, *38*, 8–11. [CrossRef]